Investigating the role of the mirn23a cluster in THP-1 human macrophage polarization

Andrew Appert[1,2,*], Richard Dahl[1,3,4,**]
[1]College of Science, University of Notre Dame
[2]Glynn Family Honors Program, University of Notre Dame
[3]Indiana University School of Medicine
[4]Harper Cancer Research Institute
[*]aappert@nd.edu
[**]richdahl@iupui.edu

Abstract

Macrophages are the primary class of phagocytic cells employed by the body's immune system, eliminating a variety of targets from foreign pathogens to cancer cells. They exist on a phenotypical spectrum: M1 macrophages are associated with tumor cytotoxicity, while M2 macrophages are known to enhance tumor viability and progression. One way in which macrophages polarize is through differential expression of microRNAs, small noncoding RNAs that post-transcriptionally regulate cell activity. We are interested in how the mirn23a cluster is responsible for producing different macrophage phenotypes, and if manipulating expression of select microRNAs can skew macrophages to the M1 tumor-cytotoxic phenotype. In this study, we generated human macrophages for the three classical phenotypes (unpolarized M0, M1, and M2) from THP-1 monocytes harboring a mirn23a cluster overexpressing vector or an empty control vector. These macrophages were analyzed for degree of polarization via qPCR to look at differences in genetic profiles of select genes associated with specific macrophage phenotypes: mannose receptor-1 (MRC1), tumor necrosis factor-α (TNFα), interleukin-6 (IL-6), and fibronectin (FN1). We hypothesized that overexpression of the mirn23a cluster would skew macrophages to show elevated levels of transcript for M1 markers TNFα and IL-6 and decreased levels of M2 markers MRC1 and FN1 relative to control macrophages. We found that overexpression of the mirn23a cluster resulted in elevated transcript levels for TNFα and IL-6 in M1 macrophages and MRC1 and FN1 in M2 macrophages; however, none of the differences in genetic profiles was statistically significant.

Introduction

Macrophages are a class of immune cells ubiquitously present in bodily tissues. Myeloid progenitor cells in the bone marrow give rise to monocytes in the blood, which mature into macrophages upon extravasation into resident tissues (Auger and Ross 2002; Mosser and Edwards 2009). Additionally, certain populations of macrophages arise from embryonic progenitors and are self-renewing (Sieweke and Allen 2013). Classically, their immunological

role is phagocytosis (Mosser and Edwards 2009), the process of engulfing and digesting cellular debris and pathogens. These cells are instrumental in mounting an immune response once pathogens invade tissues; however, they also play a number of other important roles. For example, they play an instrumental role in clearing apoptotic debris in the developing embryo (Martin et al 1994), and are involved in epithelial cell outgrowth, angiogenesis, and adipogenesis (Pollard 2009).

Because of the wide range of functions macrophages play in the body and their ubiquitous distribution, it has been suggested that macrophages exist on a phenotypic spectrum of immunoactivity ranging from classically activated, pro-inflammatory "M1" macrophages to alternatively activated, anti-inflammatory "M2" macrophages (Graff et al 2012; Mosser and Edwards 2009). In the event that an immune response is mounted, macrophages at the site of damage will polarize via extracellular signals such as interferon-γ (IFNγ) and tumor necrosis factor (TNFα) secreted by other immune cells (Mosser and Edwards 2009) to the classically pro-inflammatory M1 phenotype. Pathogenic markers such as lipopolysaccharide (LPS), a component of gram-negative bacterial cell walls, will also induce polarization to the M1 phenotype (Genin et al 2015). The M1 macrophages secrete pro-inflammatory cytokines such as IL-6 and TNFα as well as produce reactive oxygen and nitrogen species which are involved with pathogen killing (Genin et al 2015; Gordon 2003).

On the other end of the spectrum is the M2 immunological phenotype, which has been broadly described as anti-inflammatory, and is involved in the processes of angiogenesis and tissue repair (Genin et al 2015; Hagemann et al 2009). Other immune cell types are responsible for the initial secretion of extracellular signals that influence polarization to this phenotype,

releasing signaling molecules such as IL-4 and IL-13 (Genin et al 2015). IL-4 stimulates activity of the enzyme arginase in M2 macrophages, allowing these cells to convert the amino acid arginine to ornithine which itself is a precursor of the extracellular matrix component collagen (Mosser and Edwards 2009). IL-13 stimulates the expression of mannose-receptor (MRC1) on M2 macrophages (Mosser and Edwards 2009), which is involved in recognition of extracellular glycan residues.

An important difference in function between M1 and M2 macrophages is related to their interactions with tumor cells. A typical solid tumor is composed not only of malignant cells but also vasculature, host cells such as adipocytes and fibroblasts, and tumor associated macrophages (TAMs) (Genin et al 2015). Tumors recruit macrophages into the tumor microenvironment, and polarize these macrophages to the M2 phenotype. These M2-like TAMs have been shown to exhibit a number of tumor-protecting functions such as stimulation of angiogenesis, tumor cell survival and proliferation, and metastasis (Lewis and Pollard 2006). TAMs can protect the tumor against chemotherapeutic agents (Mantovani and Allavena 2015; Genin et al 2015; Shree et al 2011). On the other hand, the M1 phenotype has been shown to exhibit tumor cytotoxic activity through the release of reactive nitrogen and oxygen species and pro-inflammatory cytokines (Van Ginderachter et al 2006; Genin et al 2015). Thus, targeting polarization of TAMs constitutes a potentially novel therapeutic option in treating tumors. This potential therapeutic target is significant in the fact that it is immunologically-based, rather than focused on traditional induction of tumor cytotoxicity via radiation or chemotherapeutics, which are known to damage large numbers of healthy cells in a patient.

There are a number of intra- and extracellular factors influencing the expression of genes that lead to macrophage activation. Due to the multiple types of factors, an intermediate phenotype between the two ends of the spectrum is most likely present *in vivo*. MicroRNAs (miRNAs), small noncoding RNAs that bind to mRNA and prevent translation, constitute one such intracellular factor. MiRNAs inhibit translation by forming microRNA-induced silencing complexes (RISC) with proteins of the Argonaute family and base pairing with the 3'-untranslated region of the mRNA (Filipowicz et al 2008). Typically, the Argonaute protein within the RISC complex is catalytically active and cleaves the mRNA, rendering it untranslatable by a ribosome. Recently, these molecules have sparked interest as therapeutic options due to their potential to repolarize immune cells (Hussain et al 2018; Ma et al 2015; Lu et al 2016).

Of particular interest is the mirn23a cluster coding for three mature microRNAs: miR-23a, miR-27a, and miR-24-2. Previously our lab demonstrated that the mirn23a cluster promotes the development of myeloid cells at the expense of B cell differentiation using murine models of overexpression and germline knockout (Kong et al. 2010, Kurkewich et al. 2016). Due to the mirn23a cluster's role in cell fate decisions, this raised the question of whether or not the mirn23a cluster also plays a functional role within mature immune cell types. It has been shown that overexpression of miR-23a in murine macrophages drives the release pro-inflammatory cytokines IL-1β, IL-6, TNFα and IL-12 (Ma et al 2015), all of which are characteristic of the M1 phenotype.

In this study, we are interested in the effects of overexpression of mirn23a on the polarization of macrophages derived from the THP-1 human monocytic cell line. This cell line is

an ideal model for this study because it has been shown that when THP-1 macrophages are co-cultured with tumor cells, they exhibit behaviors similar to that of TAMs (Genin et al 2015). To determine the effects of overexpression of mirn23a, we polarized THP-1 monocytes infected with mirn23a retrovirus, isolated RNA from these cells, and analyzed the transcripts of these cells using quantitative polymerase chain reaction (qPCR) for markers of M1 and M2 polarization. We hypothesize that overexpression of mirn23a would skew THP-1 derived macrophages towards the M1 phenotype, resulting in higher levels of M1 markers TNFα and IL-6 and lower levels of M2 markers MRC1 (Stein et al 1992; Mosser and Edwards 2009) and FN1 (Gratchev et al 2001; Solinas et al 2010) relative to cells containing the empty MSCV-retroviral vector.

Materials and Methods

A. RetroVirus Manufacturing Protocol

293FT cells were grown on a 10cm plates in Dulbeccos' Modified Eagle Medium (DMEM) (Gibco™)/ 5% FBS (Atlas™)/ antibiotic/ antimycotic (AbAm, Gibco™) to be transfected with viral plasmid to produce retroviral particles. On day 1 of the virus preparation protocol 80-90% confluent 293FT cells were trypsinized, broken up, and counted using a hemocytometer. Typical counts yield 1-1.5x10^6 cells/mL media. 2 10cm plates were used per retroviral plasmid, and 5mL poly-L-lysine (Sigma) was transiently added to each plate to facilitate cell adhesion. Following poly-lysine treatment, 5mL of 0.1% gelatin was added to each plate for at least 5 minutes to ensure stickiness of the cells. Gelatin was then aspirated off plates before addition of cells. 5x10^6 cells in 8mL Opti-MEM (Gibco™)/ 5% FBS media (no AbAm) was added to each 10cm plate..

On Day 2, plasmid DNA was precipitated using 70% ethanol. 16μg of retroviral murine stem cell virus (MSCV)-mirn23a cluster plasmid or MSCV plasmid and 8μg of helper plasmid (pCL AMPHO) were precipitated for each plate. After spinning down the plasmid DNA, the ethanol was decanted and a fresh volume of 70% ethanol was added in the tissue culture hood (to avoid contamination, since this protocol does not involve antibiotics or antimycotics). After drying, the DNA pellet was resuspended in 200μL Opti-MEM. If the pellet did not resuspend well, it was inserted into a 37℃ water bath. Next, a Lipofectamine transfection was done using 45 μL Lipofectamine 2000 mixed with 1.5mL Opti-MEM in a 15mL conical. 200μL of precipitated DNA was added to a separate 15mL conical with 1.3mL Opti-MEM. After waiting 5 minutes for the Lipofectamine to dilute in the media, the diluted Lipofectamine was added

to the diluted DNA. 20 minutes were allowed to pass, and then 3mL of this mixture was added to the 10cm plate containing the 293FT cells, tilting the plate gently to mix.

On Day 3, the media was aspirated and replaced with 7mL of Opti-MEM/ 5% FBS (Atlas™). On Day 4 media containing viral protocols was collected and stored at 4℃ overnight. 7mls of fresh media was added to each plate. On Day 5, media was collected and combined with media from Day 4. Virus in the collected media was concentrated using Amicon® spin concentrators. Collected media was spun at 1500 RPM for 5 minutes to pellet cells that were accidentally removed from the plate. The supernatant was transferred to an Amicon spin concentrator and spun at 4℃ for 25 minutes at 2500 RPM. After spinning the volume of the concentrated viral supernatant was ~400ul. The virus prep was then transferred to 1.5 ml tubes in 50 ul aliquots and stored at -80℃.

B. Growing and Maintaining THP-1 Cell Cultures

THP-1 cells were cultured in RPMI 1640 media (Sigma), with 10% heat-inactivated FBS, 10mM Hepes (Gibco™), 1mM sodium pyruvate (Gibco™), 2.5g/L D-glucose (Merck), 50pM β-mercaptoethanol (Gibco™), and 1% penicillin/streptomycin antibiotics (Gibco™) . Cells were grown in 50mL flasks, in 20-25 mL of media (depending on how many cells were being plated). Media was replaced every 3-4 days, and cells were split at 1:2 or 1:3 every 2-3 days.

C. Transduction of THP-1 Cells with Retrovirus

To successfully transduce the THP-1 cells with the MSCV viral vector, a 6-well plate was coated with retronectin and plated with undifferentiated THP-1 monocytes at $1x10^6$ cells/mL. The MSCV virus was added into the wells of the plate and the cells were spinfected in the centrifuge at 3500 RPM and 30°C for 90 minutes. This spinfection step was repeated again the following day, and the cells were sorted by fluorescence activated cell sorting (FACS) for expression of green fluorescent protein (GFP) using a FacsAria III (Becton-Dickinson) cell sorter. Isolated GFP+ cells were expanded by tissue culture.

D. Differentiation Protocol

Cells were cultured and differentiated in different numbers depending on their use for isolation of RNA or cytosolic/nuclear protein. Undifferentiated THP-1 monocytes were grown up in 50mL flasks. A hemocytometer was used to quantify the number of cells: the cells were transferred to 50mL conical tubes, and 10uL of this solution was transferred to the hemocytometer for counting under a light microscope. This count multiplied by 10^4 gave the number of cells/mL of media, and multiplying by the number of mL of media gave the total number of cells. Cells being differentiated for RNA were plated at approximately $2.5x10^6$ cells over a 10cm plate.

Once plated, the monocytes were differentiated into macrophages through an initial treatment with 150nM phorbol 12-myristate 13-acetate (PMA, Sigma). The macrophages were allowed to incubate with PMA-treated RPMI media for 24 hours. The PMA-containing media was then replaced with normal growth media for 24h. 48h post-PMA treatment cytokines unique to either M1 or M2 macrophages were added to the media. Plates with monocytes differentiated into M1 macrophages were treated with 20ng/mL interferon-γ (IFN-γ, R&D Systems) and 100ng/mL lipopolysaccharide (LPS, Sigma). For M2 macrophages, plates were treated with 20ng/mL interleukin-4 (IL-4, R&D Systems) and 20ng/mL interleukin-13 (IL-13, R&D Systems).

E. Isolation and Quantification of RNA

RNA was isolated from cells using Trizol (Gibco™). Plates were washed with ice-cold 1X phosphate buffered saline (PBS). 500uL Trizol was added directly to the 10cm plates, lysing the cells. The plates were rotated for 2-3 minutes until the lysate collected in the Trizol. The lysate was transferred to a 1.5ml tube, and then 100uL of chloroform was added. The mixture was vortexed for 15 seconds, and the lysate was allowed to sit at room temperature for 2-3 minutes. The lysates were then spun at 12000g for 15 minutes at 2-8°C. This allowed for the chloroform-Trizol lysate to separate into an upper aqueous layer (in which the RNA was isolated), a DNA interphase, and a lower phenol-chloroform layer containing cellular debris. The upper aqueous layer was extracted (being very careful not to take up the interphase) and moved into a fresh 1.5 ml tube. To this fresh tube containing the aqueous RNA, 750uL of isopropanol was added to precipitate the RNA, and the tubes were stored at -20°C overnight. The next day precipitated RNA was pelleted by spinning at 12000g for 10 minutes at 4°C. The isopropanol was aspirated off, and the RNA pellets were washed twice with 500uL 75% ethanol, with another spin at 8000g and 4°C for 5 minutes between washes. After these washes the remaining ethanol was removed, and the pellets were allowed to air dry for 5-10 minutes to remove residual ethanol and purify the RNA. 25uL of RNase-free water was used to redissolve the RNA. NanoDrop spectrophotometry was used to determine the concentration of the RNA (ng/uL) and the A260/280 ratio (a marker of the purity of the RNA samples and an indicator of residual ethanol).

F. Generation of cDNA from RNA

The RNA isolated from the macrophages was then used to generate complementary DNA (cDNA) via real-time polymerase chain reaction (RT-PCR). RNA was diluted to 200ng/µL, and a master mix was generated using 10X reverse transcriptase (RT) buffer (Applied Biosystems), 100mM deoxynucleotide triphosphate (dNTP) mix (Applied Biosystems), 10X RT random primers (Applied Biosystems), MultiScribe Reverse Transcriptase (Applied Biosystems), and double-distilled water (ddH_2O). Volumes for the master mix reagents were calculated such that each 5µL RNA sample received 2.5µL RT buffer, 2.5µL random primers, 1.0µL dNTPs, 1.3µL RT, and 7.8µL ddH_2O. After the master mix was added to the RNA samples in 0.2-mL PCR tubes (USA Scientific), the samples were spun briefly and placed on an S1000™ thermocycler (BIO RAD). The protocol used to generate cDNA involved an initial heating to 25℃ for 10 minutes, then heating to 37℃ for 2 hours, and finishing with a cooling step at 4℃ for 20 minutes. cDNA was stored at -20℃ for later use.

G. Identification of Genetic Markers using qPCR

Real-time quantitative polymerase chain reaction (RT-qPCR) was used to quantify the relative numbers of transcripts for select target genes characteristic of M1 or M2 polarization. Four separate master mixes were generated using 0.5µL of target primer per sample well: PrimeTime® Mini qPCR assay (IDT) *Mrc1* exon location 27-30a, *Tnf* exon location 1b-4a, *Il-6* exon location 4-5, and *Fn1* exon location 3-4. Samples were duplexed with 0.5µL per well of primer for β-Actin (*ActB*) exon location 1-2 (PrimeTime® Mini qPCR assay, IDT) to control for unwanted variation in the amount of cDNA used between samples. 3µL per well of double-distilled water and 5µL per well of PrimeTime® Gene Expression 2X Master Mix (IDT) were added to complete the master mix. 9µL of master mix was added

to the back wall of the wells of a Multiplate® PCR Plate™ (Bio-Rad), and 1μL of cDNA was added to the front wall of each well to prevent cross-contamination. Plates were sealed with Microseal® 'B' Seals (Bio-Rad) and spun briefly to mix the cDNA and master mix.

Plates were run using a CFX96™ Real-Time System C1000™ Thermocycler (Bio-Rad) and CFX Manager software (Bio-Rad). The protocol, CFX_2stepAmp.prcl, consisted of an initial heating to 95℃ for 3 minutes (step 1), holding at 95℃ for 10 seconds (step 2), and cooling to 55℃ for 30 seconds (step 3). Steps 2 and 3 were repeated for 39 cycles. The target primers were designed with fluorophores to amplify in the FAM channel (excitation wavelength of 495nm and emission wavelength of 520nm, IDT), while the fluorophores for *ActB* transcript amplified in the Cy5 channel (excitation wavelength of 648nm and emission wavelength of 668nm, IDT).

H. Statistical Analysis

The C_t values generated from qPCR correspond to the amplification cycle stage at which fluorescence was detected by the thermocycler. For each sample within one biological replicate, a corresponding C_t value was generated in the Cy5 channel and, indicating the fluorescence of *ActB* cDNA. A ΔC_t value was generated by subtracting the *ActB* C_t value from the C_t value for the target gene. Samples were first normalized to the MSCV M0 condition by applying the average ΔC_t value of the three MSCV M0 cDNA samples to all of the other samples within the target gene. Subtraction of the average MSCV M0 ΔC_t from the individual sample ΔC_t values generated a new $\Delta\Delta C_t$ value. A power function was applied to $\Delta\Delta C_t$ in order to translate these normalized values to fold changes in cDNA for a particular target gene. These fold changes were averaged across the three triplicates for each sample to yield an average fold change in the target genes across each polarization and overexpression condition.

To analyze data across multiple biological replicates, a slightly different approach was taken in which only the C_t values relevant to our hypothesis were considered (in other words, only the C_t values of the M1 samples were compared for *Tnfα* and *Il-6*, while for *Mrc1* and *Fn1* the M2 samples were compared). Again, ΔC_t values were generated from the target gene C_t and *ActB* C_t, but in this case the samples were normalized to the MSCV condition of either the M1 or M2 phenotype depending on the gene. The next steps were identical to the data analysis within one biological replicate: generation of $\Delta\Delta C_t$, then application of a power function to translate to a fold change, and averaging triplicates. The average fold changes within single replicates were then averaged across biological replicates to yield a fold change for each phenotype/23acl overexpression condition. The standard error of the mean was taken, and an F-test was run using the average fold changes from single biological replicates. If the F-test yielded a p-value of greater than 0.05, a type-2 t-test was run using the same average fold changes. If the F-test yielded a p-value of less than 0.05, a type-3 t-test was used.

Results

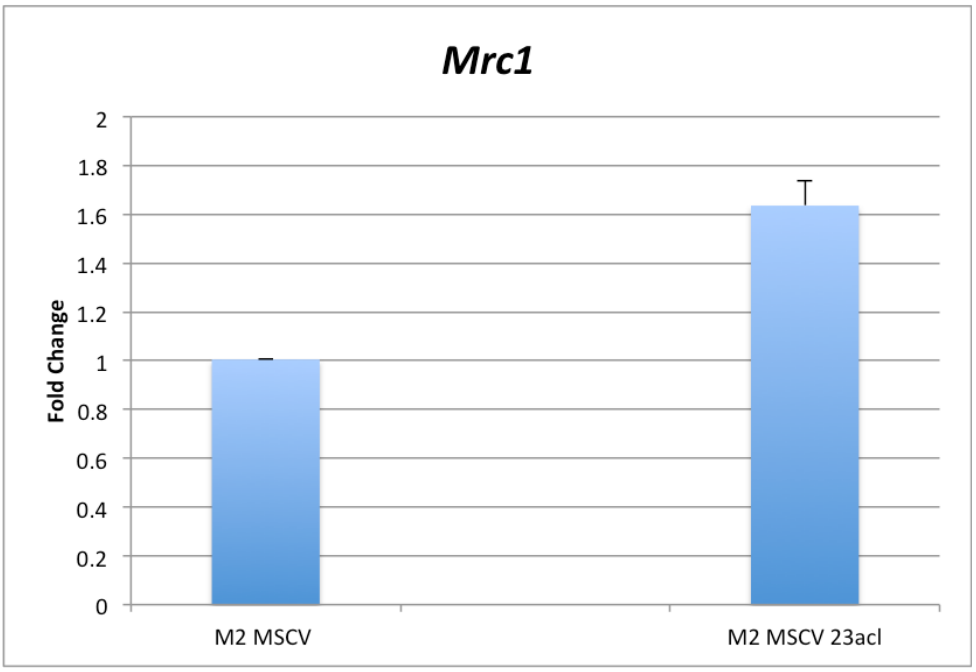

Figure 1. Fold change in transcripts from THP-1 M2 macrophages coding for MRC1, normalized to the M2 MSCV control. RNA from polarized macrophages was collected and used to generate cDNA in order to quantify the amount of transcript coding for MRC1, a marker of the M2 phenotype. Contrary to our hypothesis, the M2 macrophages with the mirn23a cluster overexpression exhibited *Mrc1* transcript levels that were higher than the control macrophages possessing the empty MSCV vector. However, the fold change relative to the control was not statistically significant (F=0.00061144, t=0.10120344). Error bars represent the standard error of the mean fold change.

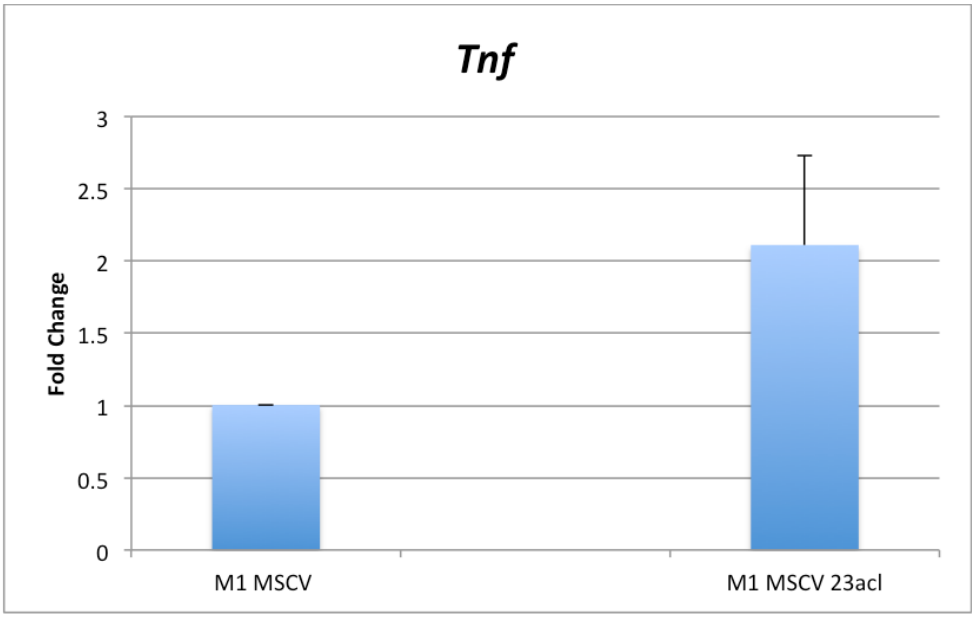

Figure 2. Fold change in transcripts from THP-1 M1 macrophages coding for TNFα, normalized to the M1 MSCV control. RNA from polarized macrophages was collected and converted to cDNA in order to quantify the amount of transcript coding for TNFα, a marker of the M1 phenotype. In accordance with our hypothesis, the M1 macrophages with the mirn23a cluster overexpression exhibited elevated *Tnfα* transcript levels compared to the control macrophages possessing the empty MSCV vector. The fold change relative to the control, however, was not statistically significant (F=0.00026288, t=0.32376534). Error bars represent the standard error of the mean fold change.

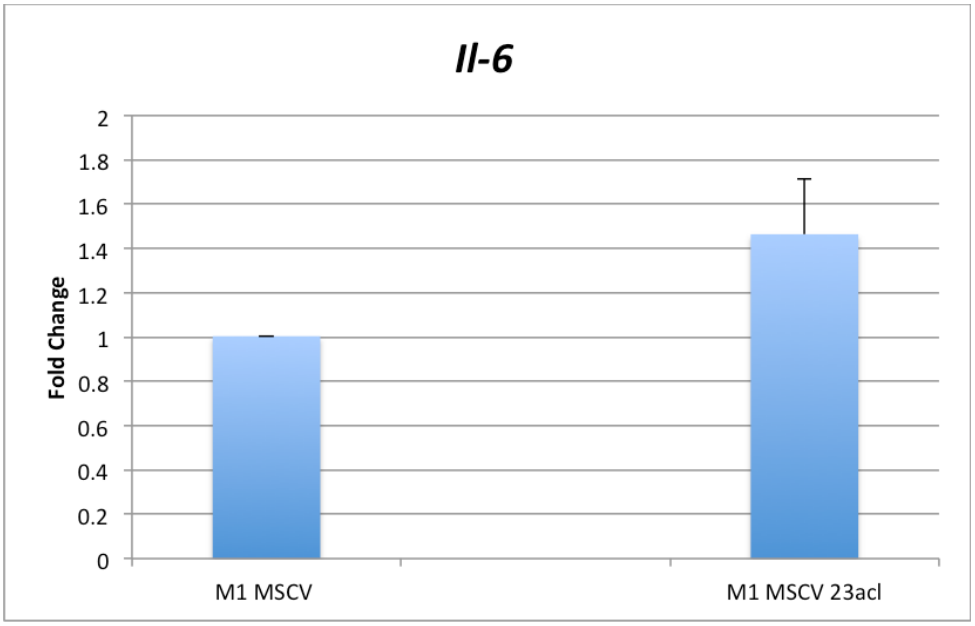

Figure 3. Fold change in transcripts from THP-1 M1 macrophages coding for IL-6, normalized to the M1 MSCV control. Isolated RNA transcripts from polarized macrophages was converted to cDNA in order to quantify the amount of transcript coding for IL-6, a marker of the M1 phenotype. As was hypothesized, M1 macrophages with the mirn23a cluster overexpression had higher *Il-6* transcript levels compared to the M1 MSCV macrophages. This fold change relative to the control was again not statistically significant (F=0.00815446, t=0.31864447). Error bars represent the standard error of the mean fold change.

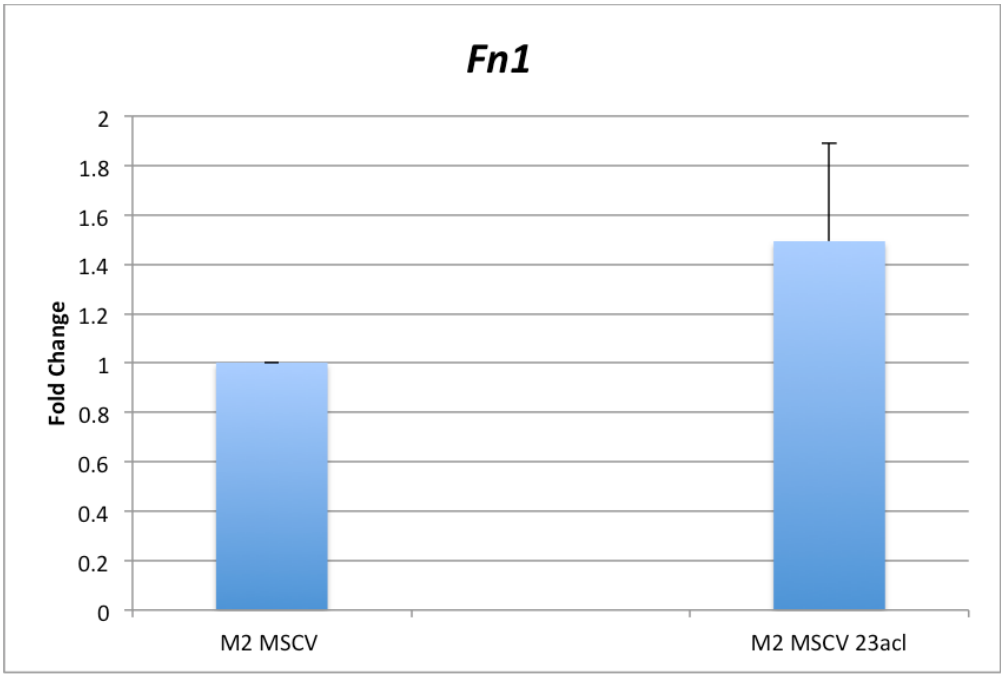

Figure 4. Fold change in transcripts from THP-1 M2 macrophages coding for FN1, normalized to the M2 MSCV control. RNA from polarized macrophages was collected and converted to cDNA for quantification of the amount of transcript coding for fibronectin, a marker of the M2 phenotype. Contrary to our hypothesis, M2 macrophages with the mirn23a cluster overexpression exhibited elevated *Fn1* transcript levels compared to control M2 MSCV macrophages; however, this fold change relative to the control was not statistically significant (F=0.00037977, t=0.43045292). Error bars represent the standard error of the mean fold change.

Because the mirn23a cluster has previously been shown to influence macrophages to release pro-inflammatory cytokines characteristic of the M1 macrophage phenotype (Ma et al 2015), it was hypothesized that overexpression of the mirn23a cluster would skew macrophages further to the M1 end of the polarization spectrum. We expected that THP-1 macrophages overexpressing the cluster would exhibit elevated levels of transcript coding for *Tnfα* and *Il-6* relative to macrophages containing the empty MSCV viral vector used to establish the overexpression. Our results indicate that the THP-1 M1 macrophages overexpressing the mirn23a cluster possessed elevated *Il-6* and *Tnfα* transcripts relative to the control M1 MSCV macrophages (Fig. 2 and 3), in line with the original hypothesis. When averaged across two

biological replicates and normalized to the M1 MSCV control, the results indicate an approximate 2.1-fold increase in *Tnfα* transcript in M1 macrophages overexpressing the mirn23a cluster (Fig. 2). The results for *Il-6* indicate a smaller increase in fold change, with the M1 mirn23a cluster macrophages showing at approximately 1.46 times the level of the M1 MSCV control (Fig. 3). While these general trends were hypothesized, the fold change in the transcripts for neither *Tnfα* nor *Il-6* was pronounced enough to reach statistical significance.

For the M2-associated proteins mannose receptor (MRC1) and fibronectin (FN1), it was hypothesized that overexpression of the mirn23a cluster in M2-polarized macrophages would result in lower levels of transcripts of these proteins relative to control M2 MSCV macrophages. The results of this study show the opposite trend, however, as transcript levels for both *Mrc1* and *Fn1* were elevated in the M2 mirn23a cluster macrophages (Fig. 1 and 4). For *Mrc1* specifically, the M2 mirn23a cluster macrophages exhibited a fold change of 1.64-times that of the M2 MSCV control (Fig. 1). The *Fn1* data showed a fold change in M2 mirn23a cluster transcript of approximately 1.49-times that of the M2 MSCV control (Fig. 4). As with the M1 data (Fig. 2 and 3), statistical analysis across the two biological replicates used to generate these results indicate no significant difference between the mirn23a cluster overexpression and MSCV control conditions.

It should be noted that these results presented display only data for the phenotype of macrophage corresponding to the hypothesis; that is, only the M2 macrophage data has been presented for M2-associated proteins (Fig. 1 and 4), and only the M1 macrophage data has been presented for the M1-associated proteins. This was done so that statistical analyses could be run across two biological replicates with fold changes normalized to the respective MSCV control

conditions. The original data collected was normalized to the M0 MSCV control condition and included fold changes for M0, M1, and M2 macrophages of both the mirn23a cluster overexpression and MSCV control conditions. These data are presented in Supplemental Figures 6-9 and are included to show that our polarization protocols were successful--one can see clear induction of M2-associated proteins in THP-1 cells stimulated with IL-4 and IL-13 (Fig. 6 and 9), and clear induction of M1-associated proteins TNFα and IL-6 (Fig. 7 and 8) in cells stimulated with LPS and IFNγ.

Discussion

In this study, we investigated the role of the mirn23a cluster on the polarization of human THP-1 macrophages. We predicted that overexpression of the mirn23a cluster would skew macrophages to the classically pro-inflammatory and anti-tumor M1 phenotype, resulting in elevated transcript levels of M1-characteristic proteins TNFα and IL-6 in M1-polarized macrophages, and decreased levels of M2-characteristic proteins MRC1 and FN1. We found that overexpression of the mirn23a cluster was associated with elevated transcript levels of both M1 markers in M1-polarized cells and M2-markers in M2-polarized cells relative to MSCV controls.

The fact that none of the fold changes are statistically significant may be explained in part due to the limitations of the study and the small amount of data collected. There were a number of issues in carrying out these experiments. Infecting the cells with the MSCV retrovirus carrying the overexpression of the mirn23a cluster was successful only after several attempts, as macrophages (being immune cells) are notoriously difficult to infect with a virus. Additionally, qPCR primers for *Actb* (β-Actin) at times failed to register fluorescence signals detectable by the thermocycler. Finally, one vial of THP-1 monocytes was contaminated, rendering any data

generated from them marred by an uncontrolled variable and the cells themselves unusable for further culturing and polarization. Due to these experimental setbacks, only two biological replicates yielded consistent data and were utilized for analysis of results, giving the results of this study weak statistical power. Even across these two biological replicates, there was great variation in the fold changes the results showed, hence the large error bars (Fig. 1-4 and 6-9) depicting the standard error of the mean.

If the trends seen in these data hold with repetition of these experiments, the results of this study must be explored in order to elucidate how the mirn23a cluster is acting from a mechanistic standpoint so that it produces elevated levels of transcripts of both M1- and M2-characteristic proteins in their respective polarization conditions. The elevated M1 markers may be explained by a previous study that has proposed the mirn23a cluster as part of a double feedback loop (Fig. 5) with key regulators of M1 polarization in the NF-κB signaling pathway (Ma et al 2015). MiR-23a, a mature microRNA contained in the cluster, is a suppressor of A20 (Ma et al 2015), a ubiquitin-editing protein responsible for regulating pro-inflammatory transcription factor NF-κB (Wertz et al 2004; Bosanac et al 2010). Because in our study we overexpressed the microRNA cluster and induced macrophage polarization to the M1 phenotype with an LPS challenge, it would make sense that pro-inflammatory NF-κB pathway would be up-regulated with greater amounts of miR-23a inhibiting A20. Thus, up-regulation of this pathway would explain why one would see higher levels of transcripts for pro-inflammatory cytokines TNFα and IL-6, since both of the genes coding for these proteins are regulated by NF-κB (Barnes and Karin 1997; Foxwell et al 2000).

Why the results of this study show elevated transcript levels of *Mrc1* and *Fn1* in M2 macrophages overexpressing the mirn23a cluster is more difficult to understand. The double feedback loop conceptualization of the mirn23a cluster's activity and regulation in M2 conditions (Ma et al 2015) indicates that the cluster's transcription is promoted by STAT6 (Fig. 5) and generally up-regulated in M2 conditions (Lu et al 2016). The feedback activity of the mature microRNAs miR-23a and miR-27a from the mirn23a cluster would be expected to down-regulate the anti-inflammatory JAK1/STAT6 pathway, limiting M2 polarization (Ma et al 2015) and inhibiting the production of M2-characteristic proteins such as MRC1 and FN1. If overexpression of the mirn23a cluster and its mature microRNAs is induced as was done in this study, one would expect a higher degree of inhibition of anti-inflammatory signaling pathways than is seen with the natural feedback activity of the JAK1/STAT6 pathway (Fig. 5).

The fact that both *Mrc1* and *Fn1* transcripts were elevated in the M2 mirn23a cluster overexpression condition certainly needs further exploration in future experiments. From a mechanistic standpoint, it may be the case that the mature microRNAs of the mirn23a cluster are involved in alternative signaling pathways involved in the production of M2-associated proteins and cytokines. Perhaps they are involved in suppression of inhibitors of signaling pathways that result in the production of MRC1 and FN1. Because the microRNA cluster codes for three individual mature microRNAs, the activities of each mature microRNA may be prevalent in different signaling pathways, and it may be the case that these pathways have opposing functions within the cell. Indeed, miR-23a and miR-27a have been implicated as having important roles in angiogenesis for highly vascularized tissues (Zhou et al 2011), a physiological process typically associated with M2 macrophages (Pollard 2009). The individualistic and cooperative roles of the

mature microRNAs coming from the cluster are undoubtedly complex and require further exploration.

It is important that this study be carried out again so that these results might be validated and carry more statistical power. If the trends seen in these data can be replicated, further studies investigating why the mirn23a cluster is capable of up-regulating transcripts for both M1- and M2-associated proteins need to be done. It may also be helpful to perform western blots and flow cytometry further assess relative levels of these M1 and M2 markers on the intracellular and cell surface protein levels, respectively. However, if the lack of statistically significant fold changes between the overexpression and control conditions holds upon repetition of this study, we may need to re-evaluate the extent of the mirn23a cluster's ability to affect signaling pathways related to macrophage polarization. After all, microRNAs have been broadly described as "fine-tuners" of gene expression and cell activity (Liu and Abraham 2013; Rajman and Schratt 2017), so it may be the case that overexpression of the mirn23a cluster may not produce the extent of skewing to the M1 phenotype that we expected, or that macrophages may have mechanisms in place to counter microRNA activity and prevent polarization too far to one end of the phenotypical spectrum. Nonetheless, microRNAs and the mirn23a cluster in particular should continue to be researched because they constitute a potential therapeutic option for the treatment of cancers from an immunological approach.

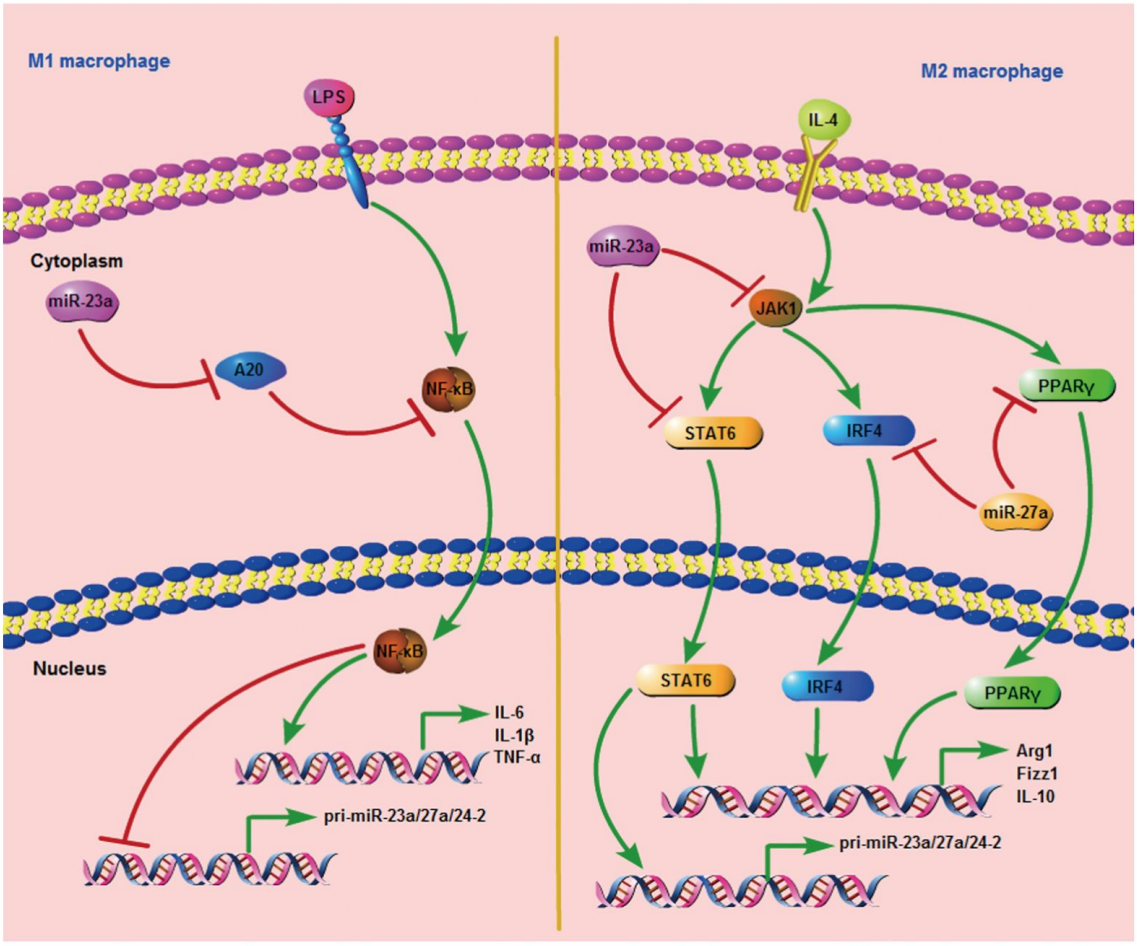

Figure 5. Signaling pathways involving the mirn23a cluster and important players regulating M1 and M2 polarization (from Ma et al 2015). A mechanistic proposal of a double feedback loop whereby the mirn23a cluster is an inhibitor of A20, a regulator of the NF-κB pro-inflammatory signaling pathway. NF-κB is itself an inhibitor of the gene coding for the immature mirn23a cluster. In the M2 case, the M2 signaling proteins are thought to up-regulate production of the immature mirn23a cluster, while the individual mature microRNAs of the cluster are thought to be inhibitors of key signaling proteins within the M2 anti-inflammatory signaling pathway STAT-6, JAK1, PPARγ, and IRF4.

Supplemental Figures

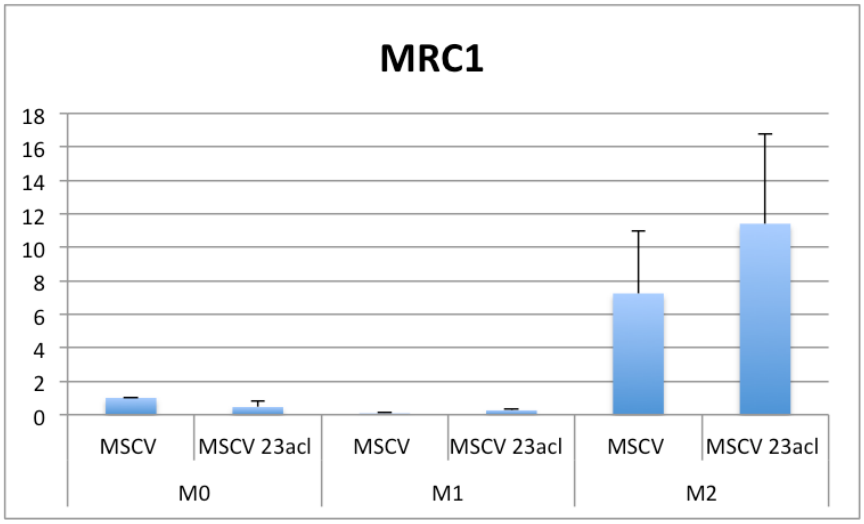

Figure 6. Fold change in transcripts from THP-1 M1 macrophages coding for MRC1, normalized to the M0 MSCV control. RNA transcripts from unpolarized M0 and polarized M1 and M2 macrophages was converted to cDNA in order to quantify the amount of transcript coding for MRC1, a cell surface protein and marker of the M2 phenotype. It is clear that our polarization protocol in this study was successful, as macrophages treated with M2 cytokines IL-4 and IL-13 exhibited highly elevated levels of MRC1 transcript. M2 macrophages with the mirn23a cluster overexpression had higher MRC1 transcript levels compared to the M2 MSCV macrophages, which did not align with our hypothesis; however, this fold change relative to the control was not statistically significant (F=0.77600722, t=0.58997043). Error bars represent the standard error of the mean fold change.

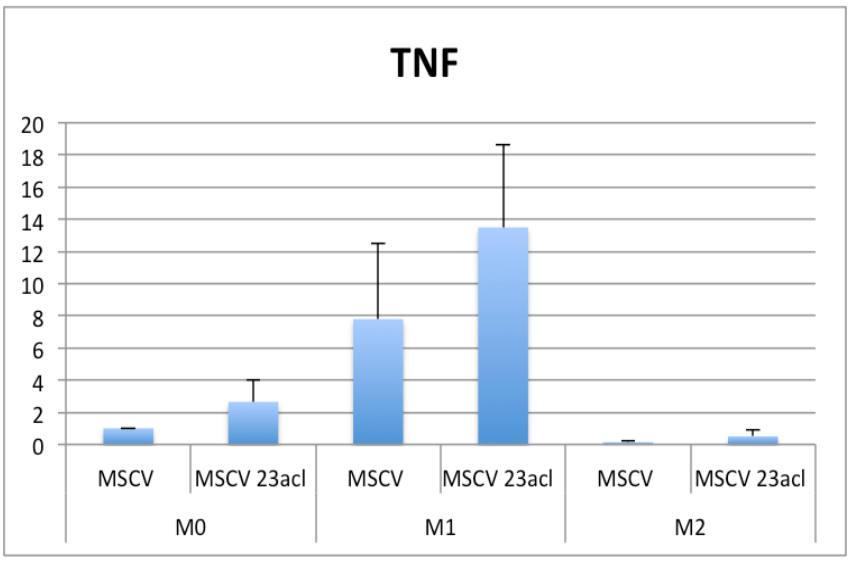

Figure 7. Fold change in transcripts from THP-1 M1 macrophages coding for TNFα, normalized to the M0 MSCV control. Isolated RNA transcripts from unpolarized M0 and polarized M1 and M2 macrophages was converted to cDNA in order to quantify the amount of transcript coding for TNFα, a pro-inflammatory cytokine and marker of the M1 phenotype. It is clear that the polarization protocol employed in this study was successful, as macrophages treated with LPS and IFNγ exhibited highly

elevated levels of *Tnfα* transcript. As was hypothesized, M1 macrophages with the mirn23a cluster overexpression had higher *Tnfα* transcript levels compared to the M1 MSCV macrophages; however, the fold change relative to the control was not statistically significant (F=0.94835759, t=0.49856437). Error bars represent the standard error of the mean fold change.

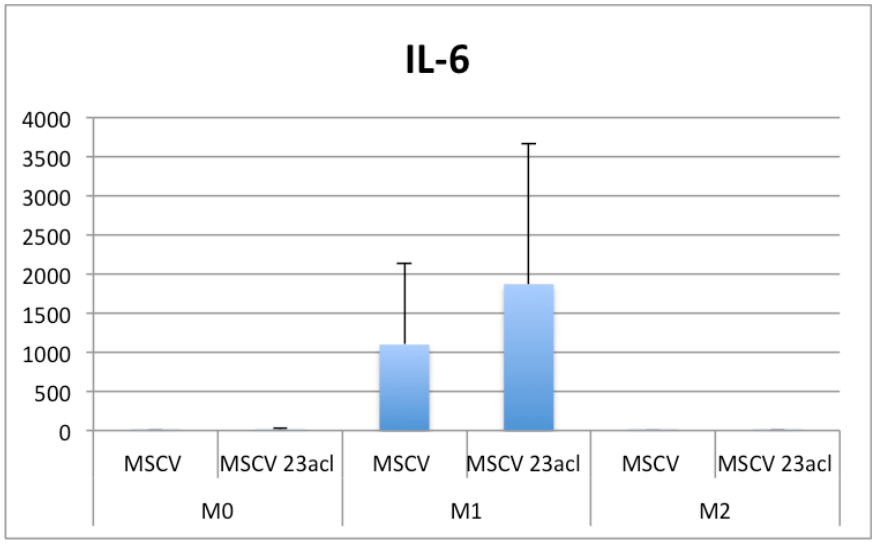

Figure 8. Fold change in transcripts from THP-1 M1 macrophages coding for IL-6, normalized to the M0 MSCV control. Isolated RNA transcripts from unpolarized M0 and polarized M1 and M2 macrophages was converted to cDNA in order to quantify the amount of transcript coding for IL-6, a pro-inflammatory cytokine and marker of the M1 phenotype. It is clear that the polarization protocol employed in this study was successful, as macrophages treated with LPS and IFNγ exhibited highly elevated levels of *Il-6* transcript. As was hypothesized, M1 macrophages with the mirn23a cluster overexpression had higher *Il-6* transcript levels compared to the M1 MSCV macrophages; however, the fold change relative to the control was again not statistically significant (F=0.67029293, t=0.74563269). Error bars represent the standard error of the mean fold change.

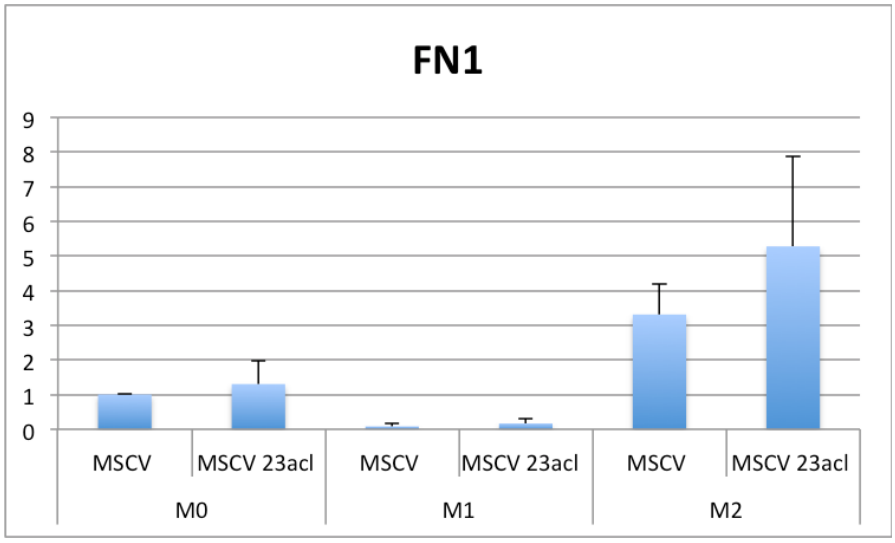

Figure 9. Fold change in transcripts from THP-1 M1 macrophages coding for FN1, normalized to the M0 MSCV control. RNA transcripts from unpolarized M0 macrophages and polarized M1 and M2 macrophages was used to generate cDNA in order to quantify the amount of transcript coding for FN1, a marker of the M2 phenotype. It is clear that our M2 polarization protocol using IL-4 and IL-13 was successful, as M2-polarized macrophages exhibit notably higher *Fn1* transcript levels. Contrary to our hypothesis, M2 macrophages with the mirn23a cluster overexpression exhibited elevated *Fn1* transcript levels compared to control M2 MSCV macrophages. This fold change relative to the control was not statistically significant (F=0.41061739, t=0.54717595). Error bars represent the standard error of the mean fold change.

Acknowledgements

I would like to thank Dr. Richard Dahl for granting me a position in his lab in which I have been fortunate enough to spend a summer and two academic years. He was kind enough to give me this independent project through which I have developed my research and writing skills greatly. His guidance and feedback in the research process and in composing this thesis have been invaluable. I would like to thank Austin Boucher for his guidance and assistance throughout the project and the writing process. Thanks as well to Harper Cancer Research Institute for providing the SURF grant that allowed me to work on this project over the summer, and finally to the Glynn Family Honors Program for affording me the opportunity to work on a senior thesis.

References

1. Ross, J.A. and Auger, MJ. The biology of the macrophage. Burke B, Lewis CE, editors. Oxford: Oxford University Press; The Macrophage. (ed 2) 2002.
2. Mosser DM, Edwards JP (2008) Exploring the full spectrum of macrophage activation. Nature Reviews Immunology 8: 958-969. DOI: 10.1038/nri2448. https://www.nature.com/articles/nri2448

3. Sieweke MH, Allen JE (2013) Beyond Stem Cells: Self-Renewal of Differentiated Macrophages. Science 342: 1242974. DOI: 10.1126/science.1242974 https://science.sciencemag.org/content/342/6161/1242974
4. Hopkinson-Woolley J, Hughes D, Gordon S, Martin P (1994) Macrophage recruitment during limb development and wound healing in the embryonic and foetal mouse. Journal of Cell Science 107: 1159-1167. http://jcs.biologists.org/content/107/5/1159.short
5. Pollard JW (2009) Trophic macrophages in development and disease. Nature Reviews Immunology 9, 259-270. DOI: https://doi.org/10.1038/nri2528. https://www.nature.com/articles/nri2528
6. Graff JW, Dickson AM, Clay G, McCaffrey AP, Wilson ME (2012) Identifying Functional MicroRNAs in Macrophages with Polarized Phenotypes. Journal of Biological Chemistry 287:21816-21825. DOI: 10.1074/jbc.M111.327031. https://www.ncbi.nlm.nih.gov/pmc/articles/PMC3381144/
7. Genin M, Clement F, Fattaccioli A, Raes M, Michiels C (2015) M1 and M2 macrophages derived from THP-1 cells differentially modulate the response of cancer cells to etoposide. BMC Cancer 15: 577-590. DOI: 10.1186/s12885-015-1546-9. https://bmccancer.biomedcentral.com/articles/10.1186/s12885-015-1546-9
8. Gordon S (2003) Alternative activation of macrophages. Nature Reviews Immunology 3: 23-35. DOI: https://doi.org/10.1038/nri978. https://www.nature.com/articles/nri978
9. Hagemann T, Biswas SK, Lawrence T, Sica A, Lewis CE (2009) Regulation of macrophage function in tumors: the multifaceted role of NF-κB. Blood 113: 3139-3146. DOI: https://doi.org/10.1182/blood-2008-12-172825. http://www.bloodjournal.org/content/113/14/3139.long
10. Lewis CE, Pollard JW (2006) Distinct role of macrophages in different tumor microenvironments. Cancer Research 66: 605-612. DOI: 10.1158/0008-5472.CAN-05-4005. http://cancerres.aacrjournals.org/content/66/2/605.long
11. Mantovani A, Allavena P (2015) The interaction of anticancer therapies with tumor-associated macrophages. Journal of Experimental Medicine 212: 435-445. DOI: 10.1084/jem.20150295. http://jem.rupress.org/content/212/4/435.full
12. Shree T, Olson OC, Elie BT, Kester JC, Garfall AL et al. (2011) Macrophages and cathepsin proteases blunt chemotherapeutic response in breast cancer. Genes & Development 25: 2465-2479. DOI: 10.1101/gad.180331.111. http://genesdev.cshlp.org/content/25/23/2465.full#aff-1
13. Van Ginderachter JA, Movahedi K, Ghassabeh GH, Meerschaut S, Beschin A et al. (2006) Classical and alternative activation of mononuclear phagocytes: Picking the best of both worlds for tumor promotion. Immunobiology 211: 487-501. DOI: https://doi.org/10.1016/j.imbio.2006.06.002. https://www.sciencedirect.com/science/article/pii/S0171298506000829#
14. Filipowicz W, Bhattacharyya SN, Sonenberg N (2008) Mechanisms of post-transcriptional regulation by microRNAs: are the answers in sight? Nature Reviews Genetics 9: 102-114. DOI: https://doi.org/10.1038/nrg2290. https://www.nature.com/articles/nrg2290#key-points
15. Hussain T, Zhao D, Shah SZA, Wang J, Yue R, Zhou X et al. (2018) MicroRNA 27a-3p Regulates Antimicrobial Responses of Murine Macrophages Infected by *Mycobacterium avium*

subspecies *paratuberculosis* by Targeting Interleukin-10 and TGF-β-Activated Protein Kinase 1 Binding Protein 2. Frontiers in Immunology 8: 1915. DOI: 10.3389/fimmu.2017.01915. https://www.frontiersin.org/articles/10.3389/fimmu.2017.01915/full

16. Ma S, Liu M, Xu Z, Li Y, Guo H, Shi J et al. (2015) A double feedback loop mediated by microRNA-23a/27a/24-2 regulates M1 *versus* M2 macrophage polarization and thus regulates cancer progression. Oncotarget 7: 2015; 7: 13502-13519. DOI: 10.18632/oncotarget.6284. http://www.oncotarget.com/index.php?journal=oncotarget&page=article&op=view&path[]=6284&path[]=16336
17. Lu L, McCurdy S, Huang S, Zhu X, Boisvert WA, Garmire LX et al. (2016) Time Series miRNA-mRNA integrated analysis reveals critical miRNAs and targets in macrophage polarization. Scientific Reports 6: 37446. DOI: 10.1038/srep37446. https://www.nature.com/articles/srep37446
18. Kong KY, Owens KS, Rogers JH, Mullenix J, Velu CS, Grimes HL, Dahl R (2010) MIR-23A microRNA cluster inhibits B-cell development. Experimental Hematology 38: 629-640. DOI: https://doi.org/10.1016/j.exphem.2010.04.004. https://www.sciencedirect.com/science/article/pii/S0301472X10001475?via%3Dihub
19. Kurkewich JL, Bikorimana E, Nguyen T, Klopfenstein N, Zhang H, Dahl R et al. (2016) The mirn23a microRNA cluster antagonizes B cell development. Journal of Leukocyte Biology 100: 665-677. DOI: https://doi.org/10.1189/jlb.1HI0915-398RR. https://jlb.onlinelibrary.wiley.com/doi/full/10.1189/jlb.1HI0915-398RR
20. Stein M, Keshav S, Harris N, Gordon S (1992) Interleukin 4 potently enhances murine macrophage mannose receptor activity: a marker of alternative immunologic macrophage activation. Journal of Experimental Medicine 176: 287–292. https://www.ncbi.nlm.nih.gov/pmc/articles/PMC2119288/
21. Gratchev A, Guillot P, Hakiy N, Politz O, Orfanos CE, Schledzewski K, Goerdt S (2001) Alternatively Activated Macrophages Differentially Express Fibronectin and Its Splice Variants and the Extracellular Matrix Protein βIG-H3. Scandanavian Journal of Immunology 53: 386-392. DOI: https://doi.org/10.1046/j.1365-3083.2001.00885.x. https://onlinelibrary.wiley.com/doi/full/10.1046/j.1365-3083.2001.00885.x
22. Solinas G, Schiarea S, Liguori M, Fabbri M, Pesce S, Zammataro L et al. (2010) Tumor-Conditioned Macrophages Secrete Migration-Stimulating Factor: A New Marker for M2-Polarization, Influencing Tumor Cell Motility. Journal of Immunology 185: 642-652. DOI: https://doi.org/10.4049/jimmunol.1000413. http://www.jimmunol.org/content/185/1/642
23. Wertz IE, O'Rourke KM, Zhou H, Eby M, Aravind L, Dixit VM et al. (2004) De-ubiquitination and ubiquitin ligase domains of A20 downregulate NF-κB signalling. Nature 430: 694-699. DOI: https://doi.org/10.1038/nature02794. https://www.nature.com/articles/nature02794
24. Bosanac I, Wertz IE, Pan B, Yu C, Dixit VM, Hymowitz SG et al. (2010) Ubiquitin Binding to A20 ZnF4 Is Required for Modulation of NF-κB Signaling. Molecular Cell 40: 548-557. DOI: https://doi.org/10.1016/j.molcel.2010.10.009. https://www.sciencedirect.com/science/article/pii/S1097276510007859?via%3Dihub

25. Barnes PJ, Karin M (1997) Nuclear Factor-κB — A Pivotal Transcription Factor in Chronic Inflammatory Diseases. New England Journal of Medicine 336: 1066-1071. DOI: 10.1056/NEJM199704103361506. https://www.nejm.org/doi/10.1056/NEJM199704103361506
26. Foxwell BMJ, Bondeson J, Brennan F, Feldmann M (2000) Adenoviral transgene delivery provides an approach to identifying important molecular processes in inflammation: evidence for heterogenecity in the requirement for NFκB in tumour necrosis factor production. Annals of the Rheumatic Diseases 59: i54-i59. DOI: http://dx.doi.org/10.1136/ard.59.suppl_1.i54. https://ard.bmj.com/content/59/suppl_1/i54
27. Zhou Q, Gallagher R, Ufret-Vicenty R, Li X, Olson EN, Wang S (2011) Regulation of angiogenesis and choroidal neovascularization by members of microRNA-23~27~24 clusters. PNAS 108: 8287-8292. DOI: https://doi.org/10.1073/pnas.1105254108. https://www.pnas.org/content/108/20/8287
28. Liu G, Abraham E (2013) MicroRNAs in Immune Response and Macrophage Polarization. Arteriosclerosis, Thrombosis, and Vascular Biology 33: 170-177. DOI: https://doi.org/10.1161/ATVBAHA.112.300068. https://www.ahajournals.org/doi/10.1161/ATVBAHA.112.300068
29. Rajman M, Schratt G (2017) MicroRNAs in neural development: from master regulators to fine-tuners. Development 144: 2310-2322. DOI: 10.1242/dev.144337. http://dev.biologists.org/content/144/13/2310.abstract